

# The Magnitude 6.7 Northridge, California, Earthquake of 17 January 1994

Scientists of the U.S. Geological Survey and the Southern California Earthquake Center

The most costly American earthquake since 1906 struck Los Angeles on 17 January 1994. The magnitude 6.7 Northridge earthquake resulted from more than 3 meters of reverse slip on a 15-kilometer-long south-dipping thrust fault that raised the Santa Susana mountains by as much as 70 centimeters. The fault appears to be truncated by the fault that broke in the 1971 San Fernando earthquake at a depth of 8 kilometers. Of these two events, the Northridge earthquake caused many times more damage, primarily because its causative fault is directly under the city. Many types of structures were damaged, but the fracture of welds in steel-frame buildings was the greatest surprise. The Northridge earthquake emphasizes the hazard posed to Los Angeles by concealed thrust faults and the potential for strong ground shaking in moderate earthquakes.

On 17 January 1994, at 4:30 a.m. Pacific standard time (12:30 UT), the first earthquake since 1933 to strike directly under an urban area of the United States occurred in a northern suburb of Los Angeles, California. This magnitude ( $M_w$ ) 6.7 (1) earthquake resulted from thrust faulting on a fault dipping down to the south-southwest beneath the northern San Fernando Valley (Figs. 1 and 2). It produced the strongest ground motions ever instrumentally recorded in an urban setting in North America and the greatest financial losses from a natural disaster in the United States since 1906. Although the Northridge earthquake was the same size as the nearby 1971 San Fernando earthquake ( $M_w$  6.7) (Figs. 1 and 2), it was much more damaging, in part because of its location directly beneath the San Fernando Valley and its closer proximity to communities in the Los Angeles basin.

The Northridge earthquake disrupted the lives and livelihoods of many of the residents of southern California. Casualties included 33 dead as a direct result of the earthquake, more than 7000 injuries treated at hospitals, and over 20,000 homeless (2). Financial losses have been estimated at \$13 billion to \$20 billion (3). Sections of three major freeways were closed, including the busiest highway in the country, Interstate 10. The losses continue to grow as damaged business districts lose customers, as time is

lost in longer commutes, and as even undamaged residential buildings lose renters in the epicentral region. In the midst of these losses, the gains made through the earthquake hazard mitigation efforts of the past two decades were obvious. Retrofits of masonry buildings helped reduce the loss of life, hospitals suffered less structural damage than in the 1971 San Fernando earthquake, and the emergency response was exemplary. The Northridge earthquake proved that preparing for earthquakes can greatly reduce the damage they do. In this article, we examine the geologic setting and the shaking and ground deformation produced by the Northridge event, analyze how they relate to the

structural damage observed, and discuss the implications of this event for earthquake hazard assessment and mitigation.

## Tectonic Setting

The causative fault of the Northridge earthquake is part of a broad system of thrust faults that result from the 160-km left step in the Pacific-North American plate boundary at the Big Bend of the San Andreas fault (Fig. 2). The northwestward motion of the Pacific plate along the San Andreas fault requires compression of the crust around this easterly bend (4). More than 10 mm/year of this compression is accommodated on east-striking thrust faults and folds of the Transverse

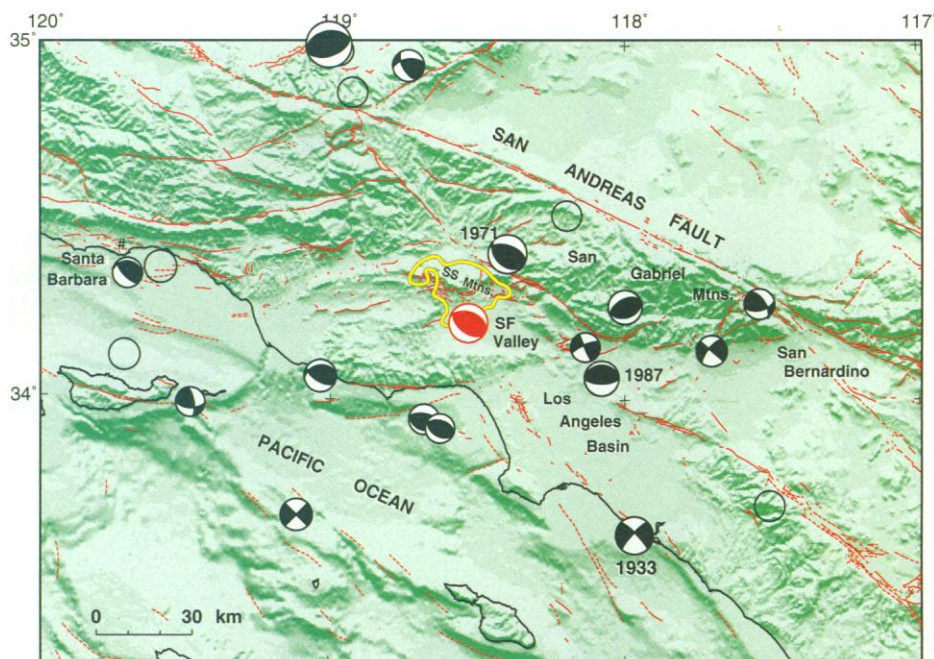


**Fig. 1.** Digital shaded relief map of southern California topography produced from United States Geological Survey (USGS) topographic data files, showing faults and  $M \geq 5.0$  earthquakes since 1932. The earthquakes are shown by lower hemisphere focal mechanisms with size proportional to magnitude, and compressional quadrants are shaded if the mechanism is known and indicated by open circles if it is not known. The mechanism of the 1994 Northridge earthquake is shown in red, and an outline of its aftershock zone is in yellow. SS, Santa Susana; SF, San Fernando.

Contributing scientists are from the University of Southern California, United States Geological Survey, California Institute of Technology, Jet Propulsion Laboratory, University of California at San Diego, California Division of Mines and Geology, and Columbia University. Direct contributions were made by L. Jones, K. Aki, D. Boore, M. Celebi, A. Donnellan, J. Hall, R. Harris, E. Hauksson, T. Heaton, S. Hough, K. Hudnut, K. Hutton, M. Johnston, W. Joyner, H. Kanamori, G. Marshall, A. Michael, J. Mori, M. Murray, D. Ponti, P. Reasenber, D. Schwartz, L. Seeber, A. Shakal, R. Simpson, H. Thio, J. Tinsley, M. Todorovska, M. Trifunac, D. Wald, and M. L. Zoback. Communications should be directed to L. Jones, U.S. Geological Survey, 525 South Wilson Avenue, Pasadena, CA 91106, USA, or K. Aki, Department of Geology, University of Southern California, Los Angeles, CA 90089, USA.

Ranges and the Los Angeles basin that we refer to as the Big Bend Compressional Zone. The zone includes many north-dipping and south-dipping subparallel faults, only some of which come to the surface (5). The interaction of these faults is not yet well understood, but no one fault dominates the deformation.

The 1994 Northridge earthquake occurred at the intersection of several mapped faults (Fig. 2) and south of the western end of the longest exposed thrust fault in the Big Bend Compressional Zone, the Cucamonga–Sierra Madre fault. This fault dips north under the San Gabriel Mountains, the steepest mountains of the belt (Figs. 1 and 2), slips at 3 mm/year (6), and produced the 1971 San Fernando earthquake (7). Fifteen kilometers west of the causative fault of the Northridge mainshock, the Sierra Madre fault system splits into two surficial faults, the north-dipping San Cayetano fault and the south-dipping Oak Ridge fault (8). The Ventura basin, the world's thickest section of Pleistocene sediments and one of the fastest-deforming

parts of California, closing at 7 to 10 mm/year (9, 10), lies between these two faults. The causative fault of the Northridge earthquake does not extend to the surface and was not mapped before the event.

The dense system of exposed and concealed thrust faults along the northern flank of the Los Angeles basin, coupled with high geodetic rates of compression, imply that the northern Los Angeles region faces one of the greatest seismic hazards in southern California (11). A report in revision at the time of the Northridge earthquake put the northern San Fernando Valley in the top one-sixth of the areas in southern California in terms of seismic potential (12). This system of faults underlies the heavily urbanized sedimentary basins, so that although each fault in this zone moves more slowly and in smaller earthquakes than is expected of the strike-slip events on the San Andreas fault, in aggregate, the seismic risk (13) from these faults may be greater.

Since 1920, 18 moderate ( $M$  4.8 to 6.7) mainshock-aftershock sequences have occurred in the greater Los Angeles area (Fig.

1) in two temporal and spatial clusters. The first was from 1920 to 1942 along the southern Los Angeles basin, whereas the second, from 1970 to the present, is concentrated along the northern edge of the Los Angeles basin (14) and involves both concealed (15) and exposed thrust faults as well as strike-slip faults in the Compressional Zone. The 1971 San Fernando earthquake ( $M_w$  6.7) (16) was located just northeast of the Northridge earthquake, also on a west-northwest-striking plane but dipping down to the north, as part of the Sierra Madre system that raises the San Gabriel mountains (Figs. 1 and 2). That earthquake (17, 18) is thought to have been bounded on the west by a northeast-striking left-lateral tear fault, called the "Chatsworth trend." Other moderate earthquakes in the most recent temporal cluster occurred on the Sierra Madre (19), Elysian Park (20), and Raymond fault systems (21). The northern flank of the Los Angeles basin has also sustained a high degree of background microseismicity in the past decade (22). Focal mechanisms in the immediate vicinity of Northridge show

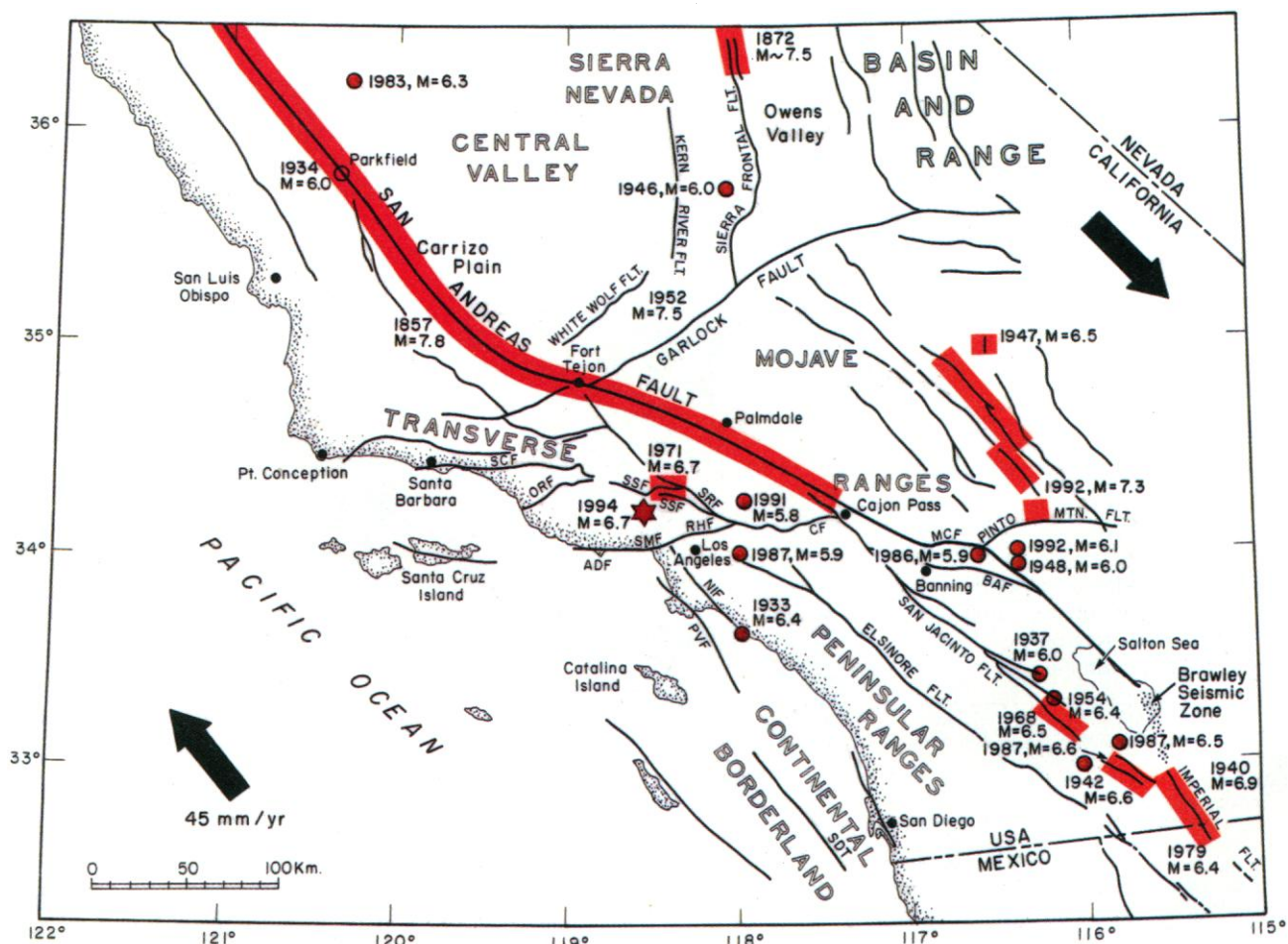


**Fig. 2.** Map of southern California showing the major faults and physiographic regions and the  $M_L \geq 6.0$  earthquakes recorded from 1932 through 1993. Historic fault rupture is shown in red. Large arrows indicate the sense and magnitude of plate motion. Some fault names are abbreviated as follows: ADF, Anacapa Dume fault; BAF, Banning fault; CF, Cucamonga fault; MCF, Mission Creek fault; ORF, Oak Ridge fault; PVF, Palos Verdes fault; RHF, Raymond Hill fault; SDT, San Diego Trough–Soledad fault; SFF, San Fernando fault; SMF, Santa Monica fault; SRF, Sierra Madre fault; SSF, Santa Susana fault; and SCF, San Cayetano fault.



thrust earthquakes in the north-dipping San Fernando rupture zone, in its westward extension, and near the Northridge mainshock fault plane. Strike-slip events continued along the Chatsworth trend (23) during this period.

## The Earthquake Source

**Mainshock source parameters.** The Northridge earthquake originated at  $34^{\circ} 12.53'N$ ,  $118^{\circ} 32.44'W$ , about 30 km west-northwest of downtown Los Angeles at a focal depth of 19 km. The first motion focal mechanism showed almost pure thrust motion on a plane striking  $N70^{\circ}W$  to  $N80^{\circ}W$  and dipping  $35^{\circ}$  to  $45^{\circ}$  to the south-southwest (Fig. 1). Models of long-period waveforms and geodetic offsets suggest similar fault orientations, although several of the longer period solutions yield a more northerly strike. The earthquake began at the southeastern corner of this plane and ruptured up to the northwest for about 15 km. This pattern suggests that rupture began on a plane striking  $N75^{\circ}W$  and bent to the north as it propagated to the west. We have no teleseismic or geodetic evidence of slip above a depth of about 8 km. Shaking from the earthquake might have been more severe in a limited area if the rupture had come closer to the

surface of the earth. The 1971 San Fernando earthquake occurred on a fault parallel to the Northridge fault but dipping in the opposite direction, down to the north. The 1994 fault dips up to the north toward the 1971 plane (Fig. 3).

Models of both body wave and surface wave data give a seismic moment of  $(1.2 \pm 0.2) \times 10^{19}$  N·m, and all the geodetic models suggest similar moments. All these models imply that the slip was greater than is normally seen for thrust faults with a rupture surface of less than  $250 \text{ km}^2$  (24). The maximum slip in the Northridge earthquake exceeded 3 m and was 5 to 10 km northwest and updip of the hypocenter. The passage of the rupture front through this region of high slip produced a distinct pulse of energy about 2 s after the start of the earthquake, leading to early media reports that the Northridge earthquake was actually two events. Because the amount of slip, and thus the seismic moment release, was large for the size of the fault, and because the duration of the event depends on the size of the fault, the seismic moment of the earthquake was released in a shorter time than is usual for an event of this size.

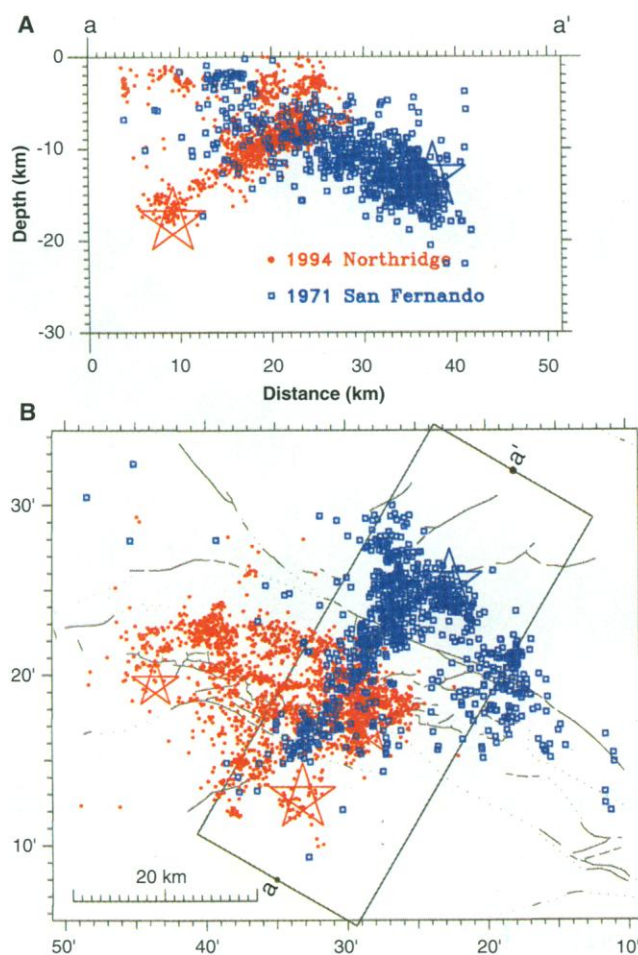
**Foreshocks.** The Northridge earthquake had no immediate foreshocks. The aftershock zone averaged 22 events per year from

1981 to 1993 that were above  $M 1.7$ , which is typical of the dispersed background seismicity in the Los Angeles region. Ten days before the event, a swarm of small earthquakes (including four  $M 3.0$  to  $3.7$ ) occurred along the coast west of Los Angeles. The alignment of the epicenters suggests that they were on a shallow south-dipping fault, parallel to the Northridge fault but offset at least 25 km to the south. Because they occurred on a separate fault, and  $M \geq 3$  events occur in the Los Angeles basin 5 to 10 times each year, we see no direct relation between these events and the Northridge earthquake.

**Aftershocks.** 3000 aftershocks of  $M > 1.5$  were recorded in the first 3 weeks of the sequence (Fig. 3) (25) in three clusters. One cluster, associated with the mainshock rupture, extends about 15 km west-northwest from the mainshock epicenter and about 15 km to the north-northeast. It defines a  $35^{\circ}$  to  $45^{\circ}$  dipping plane from a depth of 19 km to about 8 km (Fig. 3), the southern half of which is under the San Fernando Valley. The largest ( $M 5.9$ ) aftershock occurred 1 min after the mainshock, along the eastern edge of the dipping plane. A second cluster of shallower aftershocks above the dipping plane apparently reflects diffuse deformation of the overlying anticline. A third cluster, a 10-km-long group in the northwest corner of the aftershock zone, has an approximately vertical distribution beneath the Santa Susana Mountains, appearing to be on secondary faults that did not rupture in the mainshock. This cluster includes the second largest aftershock ( $M 5.6$ ), which occurred 11 hours after the mainshock at a depth of 11 km, with a thrust-faulting focal mechanism similar to that of the mainshock. This zone, including all aftershocks northwest of the  $M 5.6$  aftershock, developed only after the  $M 5.6$  event occurred. The full extent of the aftershock zone was defined by the 500 aftershocks in the first 24 hours of activity (26), and the 6300 aftershocks of the subsequent 6 months (18 January to 16 July) occurred within the same region.

Although the Chatsworth trend bounded the 1971 aftershock zone to the west (17), we do not see a similar structure in the 1994 aftershocks. Rather, the probable 1994 mainshock rupture plane extends about 15 km and is bisected by the Chatsworth trend. Northridge aftershocks occurred within the Northridge hanging wall near the Chatsworth trend; however, unlike the situation in 1971, few of the 1994 aftershocks had strike-slip mechanisms and the few that did, did not align. It thus appears that the 1994 mainshock broke across the Chatsworth trend and produced slip on both sides of that tear fault without reactivating it. Most of the 1971 aftershocks defining the Chatsworth trend were shallow ( $<10 \text{ km}$ ), so this struc-

**Fig. 3.** (A) Map of 1500 epicenters of the 1994 Northridge earthquake and its aftershocks (red) (aftershocks recorded between 17 January 1994 and 10 February 1994, with at least 30 arrival times) and of the 1971 San Fernando earthquake and its aftershocks (blue) (1971–1980) with faults from (49). Earthquakes of  $M \geq 5.5$  are shown by stars. The two largest aftershocks are at the eastern and western edges of the aftershock zone. (B) The hypocenters in the box in (A) projected onto a line trending  $N30^{\circ}E$ .





ture might exist only in the hanging wall of the 1994 earthquake.

By fitting a decay rate equation to the aftershock data from the first 12 weeks, we can estimate the number of aftershocks to expect in the future (27). The Northridge aftershock sequence has an overall productivity that is greater than average but is dying off slightly more quickly than is average for California aftershock sequences. The probability of an additional aftershock above M 5 between 1 August 1994 and 31 July 1995 is 45%.

## Earthquake Effects

**Crustal deformation.** Elastic strain released by the Northridge earthquake measurably deformed the crust over 5000 km<sup>2</sup> surrounding the epicenter. Observations of the displacements of 60 survey stations determined by means of Global Positioning System (GPS) satellites before and after the earthquake

show that the region was lifted up as much as 70 cm and displaced horizontally as much as 21 cm (Fig. 4). The earthquake raised the Santa Susana Mountains and the northern San Fernando Valley. Besides the ground motion directly attributable to slip on the fault, seven stations to the north and west of the rupture show several centimeters of westward motion that cannot be modeled by the mainshock or the major aftershocks.

Continuous high-precision strain measurements were made in boreholes at distances of 74 and 196 km from the Northridge earthquake. The coseismic, peak dynamic strains observed in the boreholes during the passage of the S waves exceeded 10 microstrain. Net offsets were 21 nanostrain of extension and 5 nanostrain of compression, which is consistent with the moment of the earthquake. No systematic change in strain above the background noise of 0.1 nanostrain occurred during the hours to mil-

liseconds before the event. Some minor relaxation occurred in the few minutes after the main rupture.

**Ground shaking.** The Northridge earthquake produced strong ground motions across a large part of the Los Angeles metropolitan area (Fig. 4). More strong motion records were obtained within 25 km of the source than had been recorded ever before for a single event. More than 200 free-field recordings were made that showed accelerations above 0.01g (28).

On average, the peak horizontal accelerations recorded in this earthquake were larger for its magnitude than those recorded for other reverse-faulting events (Fig. 5). However, how the acceleration diminishes with distance from the source in this type of earthquake had not been well established because of the paucity of data available before now, especially at very short distances. Although early reports suggested that high vertical accelerations may have con-

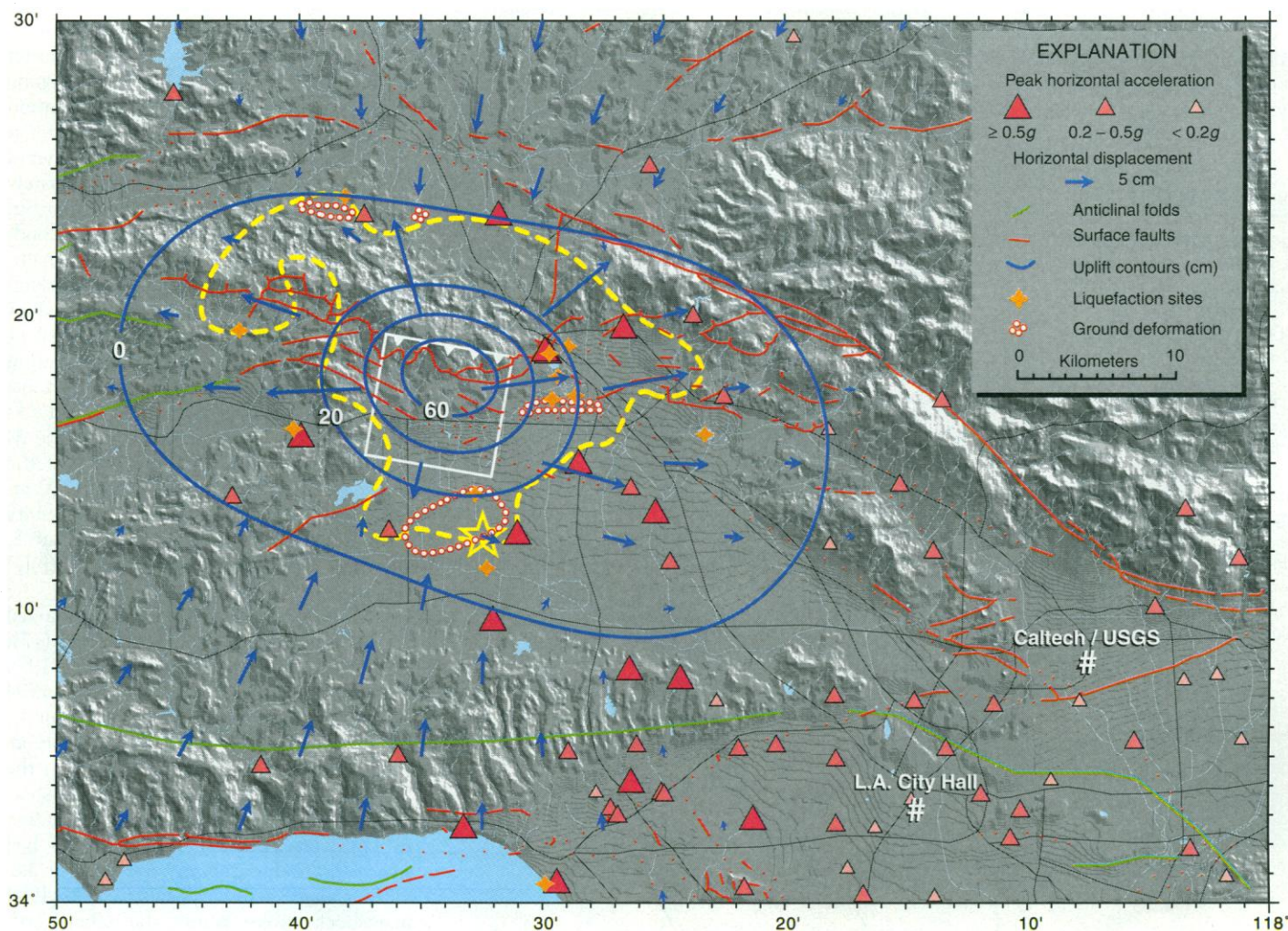


**Fig. 4.** Digital shaded relief map of southern California topography produced from USGS topographic data files showing data from the 1994 Northridge earthquake, including zones of ground deformation (red dots), contours of uplift (blue lines) and horizontal displacements (blue arrows) inferred from a model (white box) fit to the geodetically recorded deformations, most of the liquefaction sites (orange stars; some may not have been included in the early reporting), and measurements of peak ground accelerations (red to pink triangles).

tributed to the extensive damage caused by the Northridge event (an idea adopted by many who confused the vertical motion of the fault block with vertical shaking at a site), the ratio of peak vertical to peak horizontal acceleration in this earthquake is not anomalous. The vertical and horizontal ground accelerations and velocities were large, but the average peak accelerations are no more than one standard deviation above the mean of the data from other earthquakes. The high seismic moment release for a small area of fault, and thus a short duration, could have led to higher peak accelerations (29). The systematic variation in overall acceleration between earthquakes has been recognized for some time (30).

The most important factor controlling the amount of strong shaking in one event is the distance of the site from the fault plane. Sites closest to the Northridge earthquake are those north of the epicenter, because the plane is shallower to the north. Besides distance to the source, a number of other factors contributed to the variability of ground motions that is apparent in Figs. 4 and 5. Directivity (31) probably increased the ground motions at sites to the north of the epicenter as the rupture propagated toward them. In the region 10 to 15 km north-northeast of the epicenter, where we would expect the combined effects of radiation pattern (32) and directivity to be maximized for this fault geometry, the recorded ground velocities are among the largest ever recorded. The recorded peak horizontal ground velocity at a free-field site near the county hospital in Sylmar (15 km north-northeast of the epicenter) was about 130 cm/s; the peak velocity was over 170 cm/s at the Los Angeles Department of Water and Power Rinaldi receiving station several kilometers south of the hospital (33). The ground velocities in this region are dominated by a single large-

amplitude pulse that is indicative of source directivity. For many larger structures, peak ground velocity is a better measure of damage potential than is peak ground acceleration.

As in other earthquakes, soft soils may have produced larger ground motions locally (34). Several of the larger peak accelerations were located south of the epicenter, where propagation and site effects were probably more important than source radiation alone. The short duration of the peak accelerations at these sites leads to lower peak velocities as compared with the northern sites. Farther south in the northern Los Angeles basin, the generation of surface waves along the edge of the basin (35) may have played a role in the high accelerations and extensive damage caused in Santa Monica, Hollywood, and south-central Los Angeles. When data on site conditions have been collected, this earthquake will provide an opportunity to learn more about the effect of site conditions on ground motion.

**Ground rupture.** Surface deformation from earthquakes can be produced by ground rupture on the causative fault (primary faulting), displacement on nearby faults (sympathetic faulting), bedding-plane slip and extension to accommodate coseismic folding, and shaking-induced ground failures such as liquefaction and landsliding. In contrast to the 15 km of well-defined surface faulting in the 1971 San Fernando earthquake (7), the Northridge earthquake produced no clear evidence of primary surface rupture. It did, however, cause permanent ground deformation over a wide area. Along with obvious liquefaction and slope-failure features, broad zones of secondary surface ruptures were observed that are not readily attributable to common modes of shaking-induced ground failure and may in part be a response to

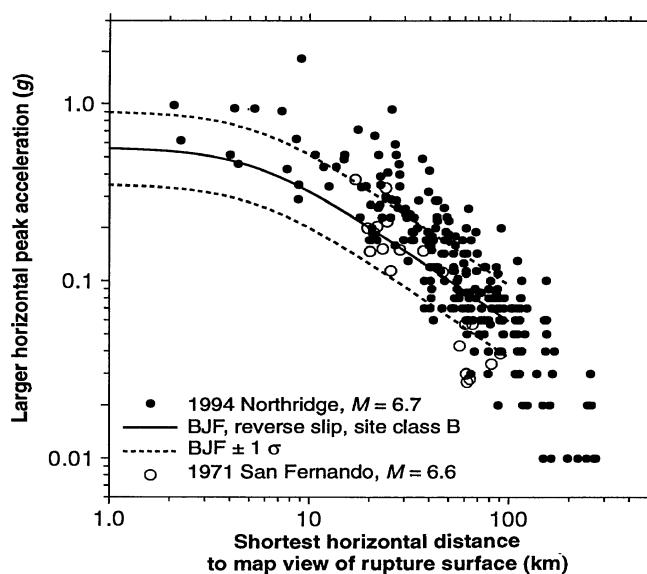
tectonic deformation. These zones were concentrated near the epicenter, in Granada Hills just east of the inferred rupture surface, and along the north flank of the Santa Susana Mountains (Fig. 4).

Most of the surface displacements observed in natural ground in these areas are extensional and cumulative displacements across zones of fractures rarely exceed a few tens of centimeters. Where these fractures cross streets and sidewalks, they are refracted into complex series of pavement cracks and buckles, spalled and extended curbs, and tented sidewalk slabs; many pavement cracks resulted from decoupling of the pavement from the ground below. Most of the surface displacements appear to be shallow and display no afterslip. They have orientations and displacements consistent with liquefaction-induced lateral spreading (36) and compaction of loosely consolidated sands within artificial fill and buried stream deposits. For these reasons, we attribute most of the deformation to ground failure from strong shaking. However, some of the features are associated with mapped faults and fold axes and may involve bedrock; thus, some features may be a response to folding during coseismic uplift of the mountains and the northern San Fernando Valley above the concealed causative fault.

Although displacements on the secondary ground ruptures are small, the linear extent of these zones is comparable to what might be expected for a surface-faulting earthquake of similar magnitude. They also caused substantial damage in densely developed areas (37). The ability to recognize zones of secondary ground deformation before the next large earthquake represents a major but not insurmountable challenge. One key may be that much deformation has occurred repeatedly in the same areas (38), and in many cases, these zones have subtle topographic expression. Secondary fractures are also commonly aligned along fault zones or axial surfaces of folds and preferentially occur in regions underlain by soft or steeply dipping sediment.

**Liquefaction.** Liquefaction produced sand blows and other evidence of permanent ground deformation in Holocene alluvial deposits and filled land at several sites within 48 km of the epicenter (Fig. 4). This deformation damaged pipelines, water supply channels, filtration facilities, parking lots, residential and commercial buildings, storm drains, and flood control debris basins. However, the Northridge earthquake caused much less ground failure due to liquefaction than many other earthquakes of its size. The near-surface deposits in the epicentral region are mainly cohesive clay and clayey silt. Such sediment is not generally susceptible to liquefaction, which might explain the relatively sparse incidence of observed liquefac-

**Fig. 5.** The larger peak of the two horizontal components of acceleration in the Northridge earthquake (filled circles) (28) compared with the median and  $\pm 1 \sigma$  curves given by the equations of (30) for a  $M_w$  6.7 earthquake and site class B (generally, very stiff soil or soft rock), which we believe represent typical Northridge sites. The acceleration data are plotted against the closest horizontal distance to the rupture defined by GPS data. We plotted only records whose motion was judged to be unaffected by structures they were on or near. The open circles show values from the 1971 San Fernando earthquake.





tion-related damage in this area. A cluster of sites 10 to 15 km northeast of the epicenter (Fig. 4) experienced liquefaction both in 1994 and in the 1971 San Fernando earthquake, but displacements at the ground surface were smaller in 1994. It is still unclear whether the smaller ground displacements resulted from compaction of soils caused by shaking, a lowered ground-water table that increased the resistance to liquefaction, the shorter duration of shaking in 1994 as compared with 1971 (39), or to engineered countermeasures taken at some sites to mitigate the liquefaction hazard.

Regional liquefaction hazard maps of the Los Angeles region are based on the assumption that highly liquefiable, loose, clay-free, sandy, alluvial fan deposits or narrow channel deposits of former streams could experience liquefaction when persistent shallow ground water is present. However, in many areas, including the western San Fernando Valley, these deposits are not mappable from surface exposure. Thus, regions of persistent shallow ground water ( $<3$  m) were mapped to highlight areas where additional site-specific studies might be advisable to determine if susceptible deposits were present (40). Additional studies of the permanent ground deformation described above are needed to determine if liquefaction-induced ground failure, settlement, or seismically induced compaction of small bodies of dry, loose sediment could explain its occurrence. For much of the epicentral area, if ground-water levels are maintained at or below present levels, the risk of liquefaction in buried channel deposits confined by nonsusceptible sediment for a comparably sized earthquake is probably low.

### Damage to Structures

Structural damage from the Northridge earthquake was extensive but not devastating. About 3000 buildings were deemed unsafe by building inspectors, which is only a small fraction of the buildings in the region of strong shaking, and many of those are repairable. Substantial failures were seen in unreinforced masonry buildings (URMs, which are primarily older brick buildings), in nonductile reinforced concrete (pre-1971 multistory commercial buildings), and in wood-frame (primarily two- to four-story apartments) and steel-frame (modern engineered buildings) buildings. Nonstructural losses, including damage to the contents of buildings, were major, probably exceeding the total cost of the structural damage. Substantial damage also occurred to bridges, a major dam, electric power facilities, and water and gas pipelines. Restoration of utilities was rapid because of the use of redundant and backup systems. The high-rises in downtown Los Angeles were outside the region of

very strong shaking and were mostly unaffected, as was the new Los Angeles subway system.

Many URMs cracked and parts of their walls fell outward, but few life-threatening collapses occurred. Many of these buildings are residential but not one life was lost, although few URMs exist in the immediate epicentral region. The San Fernando Valley had few buildings in 1933 when damage from the Long Beach earthquake inspired a change in the California building code. An URM retrofit program instituted by the City of Los Angeles in the early 1980s has strengthened 6000 buildings and undoubtedly helped to prevent loss of life during the Northridge earthquake. Damage to URMs occurred both in Los Angeles, where most of these structures have been retrofitted, and in adjacent cities without retrofit programs, so the benefits of retrofit can be studied.

Nonductile reinforced concrete buildings built before the mid 1970s, when lessons from the 1971 San Fernando earthquake were incorporated into the codes, behaved poorly, with partial collapses of a multistory medical clinic (Fig. 6) and of a mall, both high-occupancy structures during business hours. In addition, a hotel, condominium tower, hospital, and office building were severely damaged. Modern reinforced concrete structures fared fairly well, with the exception of pre-cast concrete parking garages (Fig. 6), six of which partially collapsed. Inadequate connections and poor lateral deformation capability of components intended to carry only vertical load may have contributed to these collapses.

Wood-frame buildings, both old and new, showed deficiencies. Inadequate bracing in parking areas in the ground story of multistory residential structures caused collapses

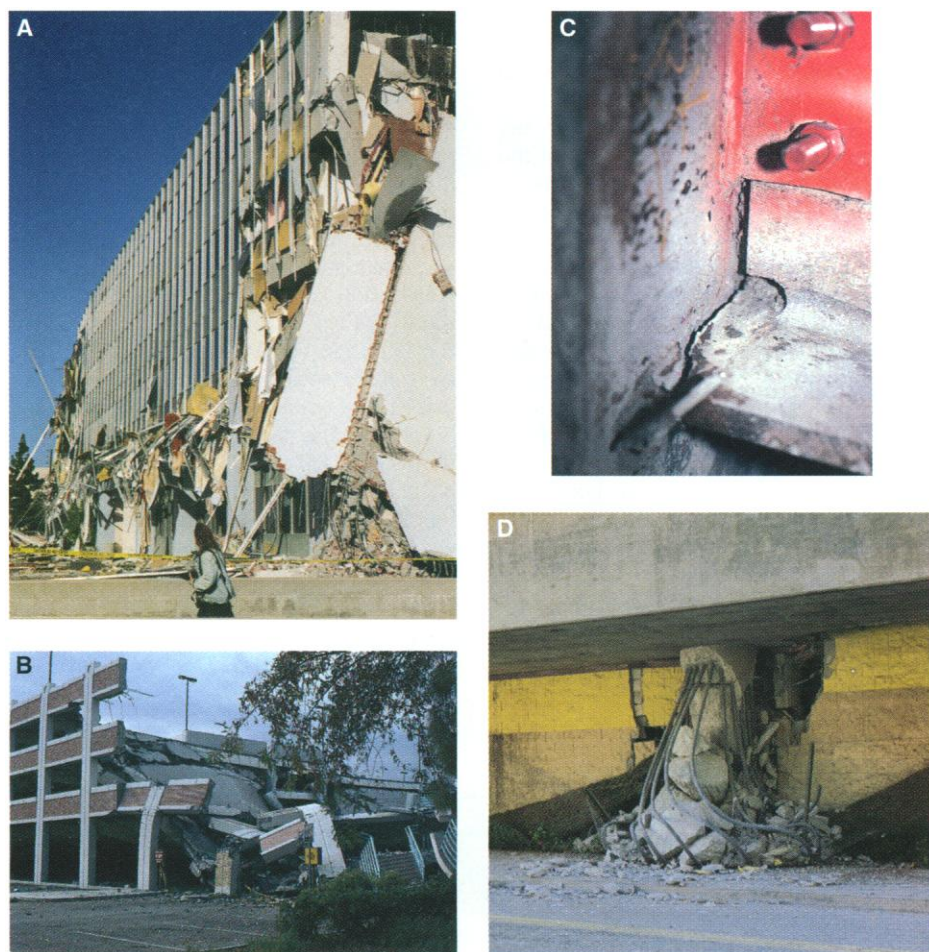


**Fig. 6.** Illustrations of structural damage from the Northridge earthquake. (A) This medical clinic in the northern San Fernando Valley is an older, nonductile concrete building. Its second story completely collapsed as did both ends of the building in the stories above. (B) The collapse of this parking garage probably originated in the interior, and the post-tensioning cables in the slabs pulled down surrounding areas. (C) A close-up photo of part of a beam-to-column joint in a steel building that suffered a weld fracture between the lower flange of the beam and the column. The bolts shown are replacements of original ones that sheared off when the lower flange weld broke. (D) This failed column supported a section of Interstate 10 and is another example of the poor behavior of nonductile concrete. The bridge deck fell onto some masonry walls of a leased storage space. (Photos courtesy of Marvin Halling [(A) and (D)] and John Hall [(B) and (C)])

of the ground story at several apartment complexes. Reliance on brittle materials such as stucco for lateral strength proved unwise as these materials broke down under cyclic loading. The modern trend toward fewer, heavier shear walls in wood-frame construction created large overturning forces and caused base anchors to fail. However, postearthquake reconnaissance of damaged wooden buildings revealed that many were not constructed according to approved plans, which suggests that a lack of proper inspection was a major reason for much damage.

The most disturbing structural behavior, with potentially great economic implications, was the brittle fracture of welded connections in steel-frame buildings, most often the beam-to-column connections (Fig. 6) that give a building its lateral earthquake resistance. The steel used in buildings is commonly believed to possess excellent ductility, but apparently the welding procedures currently in use do not achieve this desired behavior. Laboratory shaking tests sometimes show poor behavior but not to the extent seen in this earthquake. Although the problem seems serious, none of the 100 or so buildings identified as having connection fractures collapsed or even developed a serious lean. Some damaged buildings are yet to be identified, because the cracks are hidden behind fireproofing and architectural finishing materials. Many aspects of the problem, including proper repair strategies, remain to be resolved (41).

Damage to furnishings, ceilings, glass, piping, and equipment was extensive. Although hospitals are designed for higher seismic forces than are ordinary buildings, several were forced to close temporarily solely because of nonstructural damage. This included the county hospital in Sylmar, an extremely strong post-1971 structure with steel shear walls, where a peak horizontal acceleration of 2.3g was recorded on the roof in response to 0.9g shaking at the building's base. Schools suffered much nonstructural damage, and falling lights would have claimed lives had schools been in session. Water damage from broken piping required massive cleanup efforts in many buildings. Malfunctions of backup power systems affected hospitals, telephone service, and emergency response operations.

Two major base-isolated buildings were shaken by moderate ground accelerations, reaching 0.5g horizontal at one site, and performed well without damage. In this design, buildings are supported on rubber pads, which provide flexibility to isolate against horizontal ground motions. A critical design objective is to avoid excessive pad displacement, and this can be difficult if the ground motion contains a strong long-period component. Strong ground mo-

tion records at the sites of the base-isolated buildings showed only limited long-period motions, so this successful experience does not prove them fail-safe. Other sites with much larger long-period ground motions, especially the county hospital in Sylmar, would have provided a more demanding test of a base-isolated structure.

The Northridge earthquake struck during California's ongoing seismic retrofit program for bridges that began in earnest after the 1989 Loma Prieta earthquake. Altogether, about 1600 state and county bridges were subjected to shaking exceeding 0.25g. Freeway bridges in California are typically composed of reinforced concrete box girders supported on reinforced concrete columns. Seven such bridges collapsed. Five of these were of pre-1971 nonductile design and had been scheduled for retrofit, and the other two date to the mid-1970s and were of better design. One of the collapses was of a high bridge; excessive sway pulled the expansion joints apart, causing decks to fall. Inadequately reinforced columns (Fig. 6) caused the other collapses; the columns of the two more recent bridges were still substandard even though these two bridges had not been placed on the retrofit list. Several older bridges that had had their columns retrofitted by steel jackets performed well but did not experience the very strong shaking.

Of the more than 100 dams located within 80 km of the epicenter, only Pacoima Dam, an 111-m-high arch dam (located 18 km from the epicenter but only 10 km from the fault plane), suffered notable damage. Recorded accelerations as high as 2g on the canyon walls triggered numerous rock falls. A 5-cm-wide crack opened at the left abutment of the dam because of movement of the adjacent rock mass, and cracks in the upper part of the dam were a testament to the strong shaking. The water level during the earthquake was low, and because Pacoima Dam is operated for flood control, high water is infrequent. After an embankment dam liquefied and was nearly overtopped during the 1971 San Fernando earthquake, the California dam regulatory agency has overseen seismic improvements at 27 dams in the region, including the installation of rock anchors on the left abutment of Pacoima Dam that helped to limit the rock movement there during the Northridge earthquake.

### Implications for Earthquake Risk

Detailed studies of major earthquakes through the earth sciences and engineering provide us with the knowledge to mitigate future earthquake hazards. These studies include characterization of the earthquake source (using geologic, geodetic, and seismologic data to estimate how large an earthquake can occur with what probability), pre-

diction of the ground motions (given an earthquake of some size at some distance, how will the ground move under a building), and building response (how do buildings behave when subjected to those ground motions). Some of the results from the Northridge earthquake confirmed research over the past decade by the National Earthquake Hazards Reduction Program. Thrust faults concealed below Los Angeles present a threat to the region that approaches that posed by the San Andreas fault. When earthquakes occur directly beneath a city, it will be subjected to ground motions with peak accelerations approaching the force of gravity, exceeding the amounts of shaking anticipated by building codes in some respects. Some of the results, especially concerning the effects of earthquakes, reinforced findings from previous earthquakes. Ground failure induced by shaking can be as extensive as that caused by direct faulting, and the system of concealed faults under Los Angeles is more complex than previously thought, dipping both to the north and south. The severe damage done to two- to four-story residential buildings built over parking garages has important implications for regional housing needs because of the pervasive existence of such structures. Some results were a surprise. The widespread fracturing of welds in steel-frame buildings was unexpected because of the ductility of steel. Understanding the cause and correcting the problem will be essential for continued construction in earthquake-prone regions.

Because no one fault dominates the Big Bend Compressional Zone, hazard mitigation efforts that focus on avoiding one or a few fault structures are not appropriate. With scores of faults, each moving no more frequently than once or twice a millennium, the approach to mitigation must be regionally based. The most active fault need not, and probably will not, be the fault that ruptures in our lifetime. For instance, the Northridge earthquake raised the northern San Fernando Valley by several tens of centimeters, yet other earthquakes must raise the adjacent mountains at a greater rate than the valley was raised by this earthquake for the valley to be a valley. Earthquake hazard mitigation in Los Angeles must take all these faults into account.

Concealed faults beneath Los Angeles have been recognized from detailed maps of overlying geologic structures (42) and distributions of microseismicity (22). Geodetic data have been used to infer rates of motion that together with seismological or geological evidence of the location of the faults can provide an estimate of the hazard from the faults. Such studies have found several probable concealed thrust systems in the Los Angeles basin south of the San Fernando Valley. However, neither of the con-

cealed faults in the 1987 Whittier Narrows or 1994 Northridge earthquakes was recognized before the events. Our inability to recognize the causative structures before the earthquake is a testament to the inadequacies of present geologic data and the non-uniqueness of structural models. An important question is whether more detailed analyses of the San Fernando Valley before the Northridge earthquake would have allowed us to recognize that concealed fault as active before a major event. Analysis of the secondary zones of deformation produced in the Northridge earthquake may provide important constraints on models of concealed thrust faults. Recognition and analysis of such features in other regions potentially could provide a method to assess the activity and recurrence intervals of earthquakes on concealed faults.

The full extent of the urban corridor from San Bernardino through Los Angeles and northwest to Santa Barbara is at risk from both the thrust faults and the San Andreas fault, and the two risks are comparable. The earthquake history of the San Andreas fault suggests that the part of the San Andreas fault nearest to Los Angeles, the Mojave segment, produces great earthquakes on average every 131 years (43). The individual concealed and surficial thrust faults in the Big Bend Compressional Zone move more slowly, the necessary geological data are difficult to obtain in an urban setting, and the faults' earthquake history is in most cases unknown. However, geologic and geodetic estimates of slip on all the faults in Los Angeles suggest that earthquakes as large as Northridge must occur on average every 40 years somewhere in the Los Angeles region (14).

The rate of earthquakes recorded in Los Angeles since 1800 cannot account for this accumulation of slip. Three possible explanations for this discrepancy are: (i) that the rate of the past 200 years is anomalously low, and in the future, moderate earthquakes will be more common, (ii) that Los Angeles is accumulating slip to be released in an earthquake of  $M \geq 7.5$  or larger, and (iii) that significant deformation is occurring aseismically (44, 45). The rate of  $M \geq 5$  earthquakes in southern California has doubled since 1986, and the increase in Los Angeles has been even greater (46). The origins of this increase are unclear, so until we have evidence that the rate has changed again, the rate of the past decade—one  $M \geq 5$  earthquake (excluding aftershocks) per year in the Los Angeles area—should be considered the best estimate of the seismic hazard in the next few years. At this higher rate, the slip accumulated since 1800 will be relieved within 2 to 3 decades.

Slip on the Northridge fault plane undoubtedly changed the static stresses on

nearby faults, including the San Andreas fault. However, calculations suggest that if the frictional strength of the San Andreas fault is low (47), then stress changes on the fault caused by Northridge are small. The most the next large earthquake on the San Andreas fault might be delayed or advanced is 2 to 3 years, a calculation based on comparison of the magnitude of Northridge-induced stress changes with the normal tectonic loading rate for the San Andreas fault. If the nucleation point of the next southern San Andreas event is not in the region near the Northridge earthquake, then the stress change caused by Northridge is not likely to have much effect at all on the timing of that event, although post-Northridge aseismic afterslip or relaxation in the region might considerably alter the stress distribution over time.

The damage to modern buildings in the Northridge earthquake will trigger an investigation into the adequacy of the current building code in California (the Uniform Building Code). The code is based on an earthquake thought to be the largest one with a reasonable chance of occurring. The ground motion in the Northridge earthquake exceeded the design code, especially at higher frequencies. Such ground motions should be regarded as the norm near a large thrust earthquake. Moreover, this event highlighted some of the poorly understood aspects of the earthquake process, such as how an earthquake starts, how it stops, what controls the dynamic and static stress drops of an earthquake, and the effect of these variables on ground motions. Furthermore, because earthquakes larger than Northridge will occur, other deficiencies in the code may exist, such as insufficient consideration of long-period ground motion, near-fault ground motions, and duration effects. A lack of knowledge about some aspects of the behavior of structures also leads to inadequacies in the code; the fracture of steel welds is one example. However, conclusions about the code made from damage at Northridge must wait until the degree to which the code was enforced in the damaged buildings can be determined.

Because the goal of a building code is to protect life by preventing collapse, damage, sometimes unrepairable, is to be expected from strong shaking even in new structures. However, the present rate of Californian seismicity suggests that earthquakes similar to Northridge, with ground motions at the extreme of the present code, will occur several times in a structure's lifetime. Therefore, the focus of current design practice, which is solely on avoiding collapse, should be reconsidered. Engineers need to devise methods for limiting damage that can be offered as design options. Encouraging simple cost-effective mitigation mea-

sures among the public, such as securing computers, water pipes, ceiling tiles, and bookcases, could save billions of dollars in future earthquakes. Nontraditional design technologies such as base isolation show promise in reducing property losses and maintaining functionality after an event, and their development should continue.

The widespread ground failure caused by the Northridge earthquake was similar to the ground failures caused by the 1989 Loma Prieta earthquake, although in neither case did failure show any direct connection to the causative fault. These types of deformation are, in part, related to near-surface geologic conditions that can be identified and mapped for all urban areas of California. Such hazard identifications should become part of future land-use planning practices.

Almost 100 faults in the Los Angeles metropolitan area have been identified as capable of damaging,  $M \geq 6$  earthquakes (48), and more are probably still unmapped, but only a few of these (and we do not know which) will produce events in our lifetimes. Mitigation strategies for this heavily populated metropolitan area should focus on recognizing that large earthquakes in the urban areas are not rare events, on predicting the effects of these earthquakes, and on designing buildings and response strategies that adequately account for these effects.

## REFERENCES AND NOTES

1. Magnitude calculated from seismic moment ( $M_w$ ) [T. Hanks and H. Kanamori, *J. Geophys. Res.* **84**, 2348 (1979)] is considered more representative of the size of an earthquake and is 6.7 for Northridge. The local Richter magnitude, which saturates and thus underestimates the magnitude above  $M 6$ , was  $M_L 6.4$ , determined from TERRASCOPE data by H. Kanamori. The National Earthquake Information Center assigned the earthquake a 20-s surface-wave magnitude ( $M_S$ ) of 6.8.
2. J. Hall, Ed., *Northridge Earthquake January 17, 1994: Preliminary Reconnaissance Report* (Earthquake Engineering Research Institute, Oakland, CA, 1994). The dead included 20 who died from structural failures of their buildings, including 16 at the Northridge Meadows apartment complex and 13 who died from nonstructural causes such as fires, electrocution, and falls. Over 30 fatalities from heart attacks have also been attributed to the earthquake.
3. Personal communication, California Governor's Office of Emergency Services.
4. The rescaled NUVEL-1 rate for relative motion between the Pacific and North American plates at this latitude is 44.5 mm/year in the N38°W direction [poles from C. Demets, R. G. Gordon, S. Stein, *Geophys. J. Int.* **101**, 425 (1990)]. About 8 mm/year of this relative motion occurs along the Eastern California Shear Zone extending into the Basin and Range [J. C. Savage, M. Lisowski, W. H. Prescott, *Geophys. Res. Lett.* **17**, 2113 (1990)]. The remaining plate motion can be partitioned into a San Andreas fault-parallel component of 32.2 mm/year (with the use of the average N66°W trend of the San Andreas fault directly adjacent to Northridge) and a fault-normal component of 17.1 mm/year in a N24°E direction.
5. The understanding of this system is rapidly evolving as new results are obtained, so no one paper provides a definitive overview. The surface geology is described in (48) and the seismotectonics in (22).
6. R. J. Crook, C. R. Allen, B. Kamb, C. M. Payne, R. J. Proctor, *U.S. Geol. Surv. Prof. Pap.* **1339**, 27 (1987).



7. U.S.G.S. staff, *ibid.* **733**, 55 (1971).
8. R. S. Yeats, *J. Geophys. Res.* **88**, 569 (1983).
9. A. Donnellan, B. H. Hager, R. W. King, *Nature* **366**, 333 (1993).
10. R. S. Yeats, *J. Geophys. Res.* **93**, 12137 (1988).
11. S. Ward, *Bull. Seismol. Soc. Am.* **84**, 1293, (1994); S. G. Wesnousky, *J. Geophys. Res.* **91**, 12587 (1986).
12. The Northern San Fernando Valley was in the top one-sixth in terms of the potential for moment release from earthquakes of  $M \geq 6.5$  [D. Jackson, *Seismol. Res. Lett.* **65**, A5 (abstr.) (1994)]. The region was assigned a high value because of its high geodetic rates of closure.
13. Seismic risk is defined as the hazard times the exposure, where hazard is the potential for damaging earthquake shaking, and exposure is the number of potentially damagable structures in that region.
14. E. Hauksson, in *Engineering Geology Practice in Southern California* (Southern California Section, Association Engineering Geology, Belmont, CA, 1992), p. 167.
15. Concealed faults (sometimes called blind faults) are faults that do not crop out at the earth's surface but instead are capped by folds that accommodate the fault's slip in nonbrittle deformation. The slip rates on these faults can be inferred from the growth rates of the overlying folds [R. S. Stein and G. C. P. King, *Science* **224**, 869 (1984)] (18).
16. This moment magnitude is based on T. Heaton's moment of  $1.3 \times 10^{19}$  N-m [Bull. Seismol. Soc. Am. **72**, 2037 (1982)]. The local magnitude of the 1971 event was 6.4, the same as for Northridge.
17. T. C. Hanks, *J. Geophys. Res.* **79**, 1215 (1974).
18. J. H. Whitcomb, U.S. Geol. Surv. Prof. Pap. **733**, 30 (1973).
19. The 1991 Sierra Madre earthquake was  $M$  5.8 [E. Hauksson, *Bull. Seismol. Soc. Am.* **84**, 1058 (1994)].
20. "Elysian Park fault system" and "Santa Monica Anticlinorium" have both been used to describe some or all of the concealed faults along the north-to-northeastern flank of the Los Angeles basin. As defined in (22), the Elysian Park system has included the 1987 Whittier Narrows ( $M$  5.9) earthquake [E. Hauksson and L. M. Jones, *J. Geophys. Res.* **94**, 9569 (1989)] (45) and the 1979 ( $M$  5.2) and 1989 ( $M$  5.0) Malibu earthquakes [E. Hauksson and G. M. Saldivar, *ibid.*, p. 9591].
21. The earthquake on the Raymond fault system was the 1988 ( $M$  5.0) Pasadena earthquake [L. M. Jones, K. E. Sieh, E. Hauksson, L. K. Hutton, *Bull. Seismol. Soc. Am.* **80**, 474 (1990)].
22. E. Hauksson, *J. Geophys. Res.* **95**, 15365 (1990).
23. These results are from a study of small earthquakes in the region from 1980 to 1992 [L. Seeber, *Seismol. Res. Lett.* **65**, A10 (abstr.) (1994)].
24. Slip on a concealed fault plane must be inferred from indirect measurements. Data from many sources, including seismological body and surface waves, local strong ground motions, displacements measured by the GPS, and leveling lines can be inverted to estimate the distribution of slip. The details of the distribution vary depending on the data sets and model assumptions. The results in the text are the robust features common to all of the models so far.
25. The aftershock data were collected and analyzed by the Southern California Seismographic Network operated by the California Institute of Technology and the U.S. Geological Survey.
26. Unlike the situation after the larger 1992 Landers earthquake [D. P. Hill *et al.*, *Science* **260**, 1617 (1993)], no widespread increase in seismicity was observed at regional distances after the Northridge mainshock. However, within the coda of the Northridge mainshock, a few small ( $M < 1$ ) events were observed at Medicine Lake, east of the Long Valley Caldera, and in The Geysers geothermal area. The Geysers geothermal field has shown increased seismicity after 6 regional events but not after 22 others, depending on the distance to the mainshock and the mainshock magnitude [S. D. Davis, *Eos* **74**, 317 (abstr.) (fall 1993)]. The Geysers region has a high, fairly constant degree of seismicity, which suggests that it is in a metastable condition and thus is prone to triggering by small perturbations such as the dynamic shaking of regional events. Northridge should have been too small to have triggered a swarm, so other factors may be important.
27. P. Reasenberg and L. Jones [Science **243**, 1173 (1989)] showed that the rate at which aftershocks occur after mainshocks can be described by  $\lambda(t, M) = 10^{[a + b(M_m - M)](t + c)^{-p}}$ , where  $\lambda$  is the rate,  $t$  is time,  $M$  is the magnitude of an aftershock,  $M_m$  is the magnitude of the mainshock, and  $a$ ,  $b$ ,  $c$ , and  $p$  are constants ( $a$  is the overall productivity of the sequence,  $b$  is the frequency of magnitudes,  $p$  is the rate at which the aftershocks decay with time, and  $c$  is the time delay until the sequence starts to decay). Once these four parameters are determined for a sequence, the rate of aftershocks is fully described, and the probability of future aftershocks can be determined. The parameters for Northridge are almost exactly average for California aftershock sequences except for the high overall productivity,  $a$ . For Northridge,  $a$  is  $-1.3$ ,  $b$  is  $0.90$ ,  $c$  is  $0.09$  days, and  $p$  is  $1.2$ . The Californian average is  $a$ ,  $-1.67$ ;  $b$ ,  $0.91$ ;  $c$ ,  $0.05$  days; and  $p$ ,  $1.08$ . For the 1971 San Fernando earthquake,  $a$  is  $-2.2$ ,  $b$  is  $1.08$ , and  $p$  is  $1.2$ . For the 1933 Long Beach earthquake,  $a$  is  $-1.0$ ,  $b$  is  $1.0$ , and  $p$  is  $1.3$ .
28. A. Shakal *et al.*, California Strong Motion Instrumentation Program, Office of Strong Motion Studies Report 94-07 (1994); R. Porcella, E. Etheredge, R. Maley, A. Acosta, U.S. Geological Survey Open-File Report 94-141 (1994); M. D. Trifunac, M. I. Todorovska, S. S. Ivanovic, *Int. J. Soil Dyn. Earthquake Eng.*, in press.
29. T. C. Hanks and R. A. McGuire, *Bull. Seismol. Soc. Am.* **71**, 2071 (1981); D. M. Boore, *ibid.* **73**, 1865 (1983); *ibid.* **76**, 43 (1986). These studies model the earthquake source in terms of moment and a term called the stress parameter, which controls the dynamic ground motion amplitudes. A model of Northridge data with a frequency-dependent attenuation  $Q$  [ $Q = 61 \times \omega$  (Hz)], from an earlier analysis of the San Fernando earthquake [A. Papageorgiou and K. Aki, *ibid.* **73**, 953 (1983)] compared the observed peak horizontal accelerations at rock sites with those predicted for a single  $\omega$ -squared model with  $f_{max} = 10$  Hz with the use of the site amplification factor estimated by the coda method [F. Su *et al.*, *ibid.* **82**, 580 (1992); B. H. Chin and K. Aki, *ibid.* **81**, 1859 (1991)]. The "stress parameter" of the best-fitting model was about 150 bars, which is more than twice the representative value for the western United States [G. Atkinson and D. Boore, *Earthquake Spectra* **6**, 15 (1990)].
30. D. M. Boore, W. B. Joyner, T. E. Fumal, U.S. Geological Survey Open-File Report 93-509 (1993); W. B. Joyner and D. M. Boore, *Bull. Seismol. Soc. Am.* **71**, 2011 (1981); D. R. Brillinger and H. K. Preisler, *ibid.* **74**, 1441 (1984); *ibid.* **75**, 611 (1985).
31. The velocity of rupture propagation is close to the velocity of shear-wave propagation. As a consequence, if rupture propagates toward a station, radiation from a relatively long portion of the rupture arrives at the station in a relatively short time as compared with stations at other azimuths, hence the ground motions are larger. A station located in the opposite direction will record a more elongated wave train with less severe ground motion.
32. The shear motion across a fault leads to a nonhomogeneous distribution of energy radiation from an earthquake. Santa Monica was in the direction of maximum S wave radiation, whereas Pasadena was at a minimum in both  $P$  and  $S$  waves.
33. Velocities are determined from integration of acceleration records. A glitch in the film record at the Rinaldi station, interpreted as a stall in the advancing mechanism, makes the temporal integration uncertain. The value of 170 cm/s assumes that the film stalled for 0.05 s. Assuming no stall gives a minimum estimate of 130 cm/s. Any longer delay would imply an even higher velocity.
34. The most extreme local geologic site effect in the Northridge earthquake was at a site in Tarzana with a peak horizontal acceleration of 1.82g. In the 1987 Whittier Narrows earthquake, the same site had a peak horizontal acceleration of 0.62g, which is more than 10 times greater than the geometric mean of seven sites at similar distances. In other events, including a Whittier Narrows aftershock, the peak horizontal acceleration at this site was not especially large. Because the nearby nursery and homes in the area did not experience unusually great damage, the large peak acceleration must have been caused by very localized amplification.
35. T. C. Hanks, *Bull. Seismol. Soc. Am.* **65**, 193 (1975); L. A. Drake, *ibid.* **70**, 571 (1980); H.-L. Liu and T. H. Heaton, *ibid.* **74**, 1951 (1984); J. E. Vidale and D. V. Helmberger, *ibid.* **78**, 122 (1988).
36. Many extensional fractures and grabens parallel contours, exhibiting displacements consistent with movement down a gradual slope. However, unequivocal evidence for liquefaction, such as the venting of sand and water to the surface, was not observed in association with these ground fractures except for a few isolated occurrences in Potrero Canyon, along the north flank of the Santa Susana Mountains. Studies are in progress to assess whether much of the deformation could have resulted from liquefaction at depth that did not expel sand.
37. Ground fractures were the cause of numerous breaks in water and gas lines, including the rupture and explosion of a 22-inch gas main that destroyed five homes. Ground failure was also wholly or partially to blame for extensive foundation damage to hundreds of homes in the San Fernando Valley.
38. Several trenches excavated across normal faults along the south margin of Potrero Canyon reveal evidence for two earlier displacement events that were equal in size to the  $\sim 28$ -cm displacement produced there by the Northridge earthquake. Whether tectonic or induced by shaking, these observations indicate that this area experienced at least two earthquakes in the late Holocene with ground motions similar to that of the Northridge earthquake. Preliminary radiocarbon dates suggest that the penultimate event occurred within the past 1200 years.
39. The duration of rupture in the 1971 earthquake was 10 to 12 s [T. Heaton, *ibid.* **72**, 2037 (1982)] as compared with 6 to 8 s for the Northridge earthquake. Each shaking cycle increases the compaction of soils, so that duration is an important factor controlling liquefaction [T. L. Youd, *J. Soil Mech. Found. Eng.* **98**, 709 (1972)].
40. J. C. Tinsley, T. L. Youd, D. M. Perkins, A. T. F. Chen, U.S. Geol. Surv. Prof. Pap. **1360**, 263 (1985).
41. Earthquake damage is cumulative, with each cycle of loading increasing the likelihood of damage and collapse. Failure to repair damage from this earthquake will increase the chance of life-threatening damage in the next event.
42. R. S. Yeats, in preparation; T. L. Davis and J. Namson, in preparation; T. L. Davis, J. Namson, R. F. Yerkes, *J. Geophys. Res.* **94**, 9644 (1989).
43. K. E. Sieh, M. Stuiver, D. Brillinger, *J. Geophys. Res.* **94**, 603 (1989). The last earthquake on this segment was in 1857.
44. R. S. Stein and R. S. Yeats, *Sci. Am.* **260**, 48 (June 1989).
45. J. Lin and R. S. Stein, *J. Geophys. Res.* **94**, 9614 (1989).
46. Since 1900, moderate ( $M > 4.8$ ) earthquakes in the Los Angeles region have occurred in two clusters, with 5 events between 1920 and 1942 and 10 events so far since 1970. No moderate events were recorded between 1942 and 1970 (14). Previous changes in the rate of moderate earthquakes in California have in some cases been followed by major earthquakes [such as the 1906 ( $M$  8) San Francisco, 1983 ( $M$  6.5) Coalinga, and 1989 ( $M$  7.1) Loma Prieta events]. In other cases, such as the Long Valley area from 1978 to 1986 and the Banning region of southern California from 1935 to 1948, no event within the cluster was significantly larger than the others. In the earlier Los Angeles cluster, the largest event ( $M$  6.4, at Long Beach) was in the middle of the group. The mechanisms controlling rate changes or their relation to the largest earthquakes of a region are not understood.
47. M. D. Zoback *et al.*, *Science* **238**, 1105 (1987).
48. J. I. Ziony and R. F. Yerkes, U.S. Geol. Surv. Prof. Pap. **1360**, 43 (1985).
49. C. W. Jennings, *Fault Map of California with Volcanoes, Thermal Springs and Thermal Wells (Scale 1:750,000)*, California Division of Mines Geology, Geologic Data Map No. 1 (1975).
50. We thank W. Ellsworth and R. Page for insightful and constructive reviews. Sponsored by NSF through the Southern California Earthquake Center, the U.S. Geological Survey, and NASA.